Supporting Information

Tuning effect of the zeolite Brønsted acidity on the FeZn bimetallic hydrodesulfurization catalyst

Wenkai Wei,[†] *Xinyue Zhang,*[†] *Xuandong Liu,*[†] *Rong Guo,*[†] *Bo Meng*[†], *Guosheng Li*[†], *Shenyong Ren*[†], *Qiaoxia Guo,*[§] *Baojian Shen*[*,†]

[†]State Key Laboratory of Heavy Oil Processing; the Key Laboratory of Catalysis of CNPC; College of Chemical Engineering and Environment, China University of Petroleum, No. 18 Fuxue Road, Changping, Beijing 102249, China

[§]College of Sciences, China University of Petroleum, No. 18 Fuxue Road, Changping, Beijing 102249, China

*Corresponding Author: Baojian Shen

TEL: +(8610)89733369

FAX: +(8610)89733369

EMAIL: baojian@cup.edu.cn

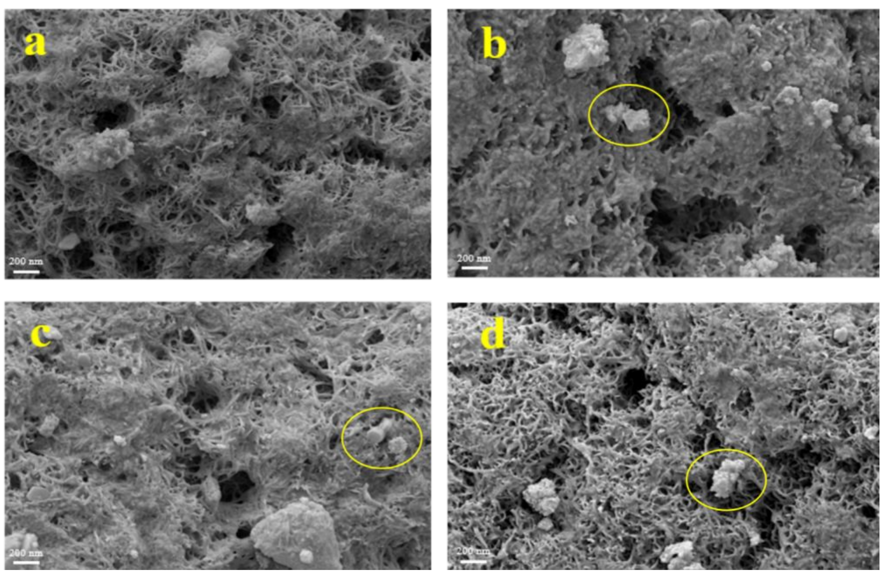

Figure S1. SEM images of (a) PA, (b) PSA10, (c) PSA18 and (d) PSA24 supports.

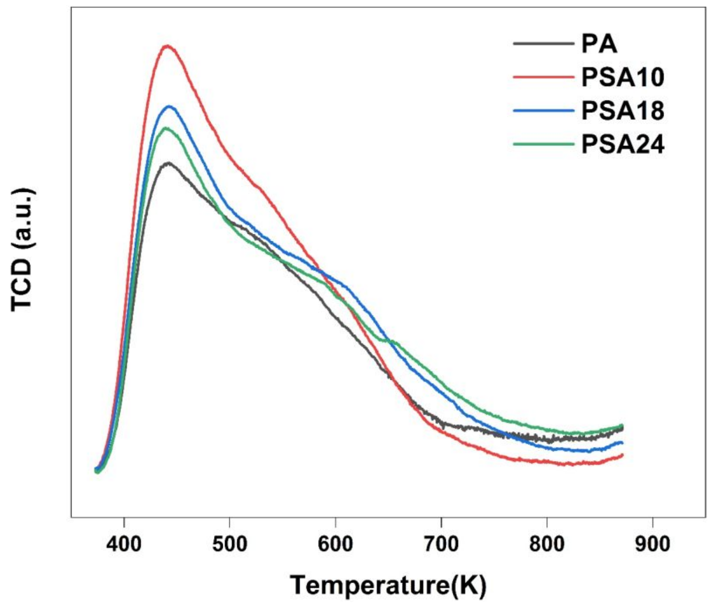

Figure S2. NH_3-TPD profiles of supports.

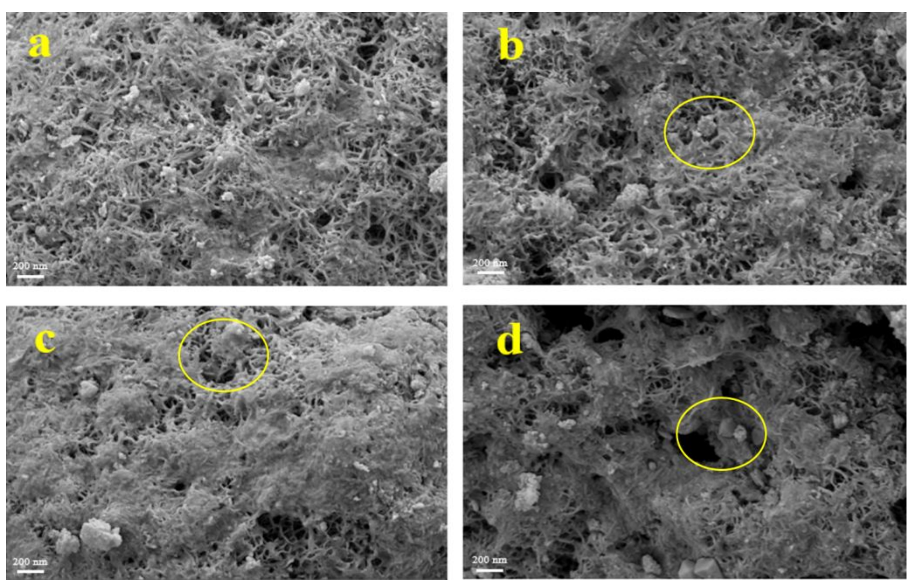

Figure S3. SEM images of (a) FZ-PA, (b) FZ-PSA10, (c) FZ-PSA18 and (d) FZ-PSA24 oxide catalysts.

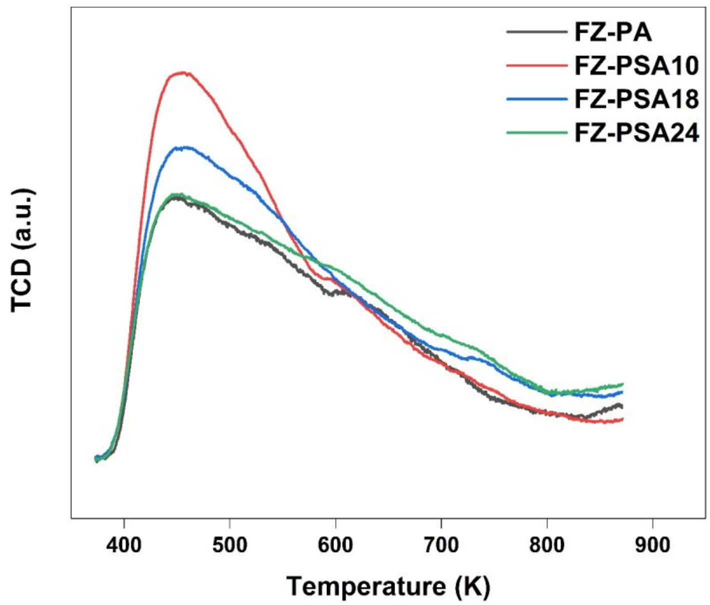

Figure S4. NH_3-TPD profiles of catalysts in oxide form.

Table S1. Detailed texture properties of supported FeZn catalysts before H_2-reduction

Supports	S_{BET} /($m^2 \cdot g^{-1}$)	S_{Micro} /($m^2 \cdot g^{-1}$)	S_{EXT} /($m^2 \cdot g^{-1}$)	V_P /($cm^3 \cdot g^{-1}$)	V_{micro} /($cm^3 \cdot g^{-1}$)	V_{meso} /($cm^3 \cdot g^{-1}$)	D_{aver} /nm
FZ-PA	251	26	225	0.785	0.011	0.774	12.52
FZ-PSA10	313	136	177	0.649	0.066	0.583	8.31
FZ-PSA18	301	133	168	0.630	0.064	0.566	8.38

FZ-PSA24	302	126	176	0.617	0.060	0.557	8.17

Table S2. Composition of supported FeZn catalysts before H_2-reduction

Catalysts	Composition of the catalysts(wt%, XRF)			Composition of the catalysts(wt%, ICP)		
	Fe_2O_3	ZnO	Support	Fe_2O_3	ZnO	Support
FZ-PA	9.0	12.7	78.3	9.4	13.0	77.6
FZ-PSA10	9.1	13.1	77.8	9.6	13.5	76.9
FZ-PSA18	9.1	12.8	78.1	9.3	13.3	77.4
FZ-PSA24	9.0	13.0	78.0	9.5	13.4	77.1

The Py-IR characterization of the fresh and spend catalyst was performed and the spectra were presented in **Figure S5**. It is apparent that the characteristic peak around 1543 cm^{-1} belongs to the Brønsted acid sites and the peak at 1453 cm^{-1} is attributed to the Lewis acid sites. It is obvious that the peak intensity of the spend catalyst FZ-PSA18 is weaker than that of the fresh catalyst FZ-

PSA18. The densities of Brønsted and Lewis acid sites in catalyst can be calculated in **Table S3**. After reaction, the total amount of B acid and L acid dropped from 20 to 8 μmol/g, 149 to 74 μmol/g, respectively. This is due to the formation of coke on the catalyst. The SEM-EDS spectra of fresh catalyst FZ-PSA18 and spend catalyst FZ-PSA18 catalysts were presented in **Figure S6**. Compared with fresh catalyst FZ-PSA18, the carbon content in the spend catalyst FZ-PSA18 catalyst increased significantly from 5.4 to 31.8 wt%, which is consistent with the Py-IR result. These results indicate that under the experimental conditions of this article, the introduction of Y-type zeolite will cause the obvious coke deposition of the catalyst.

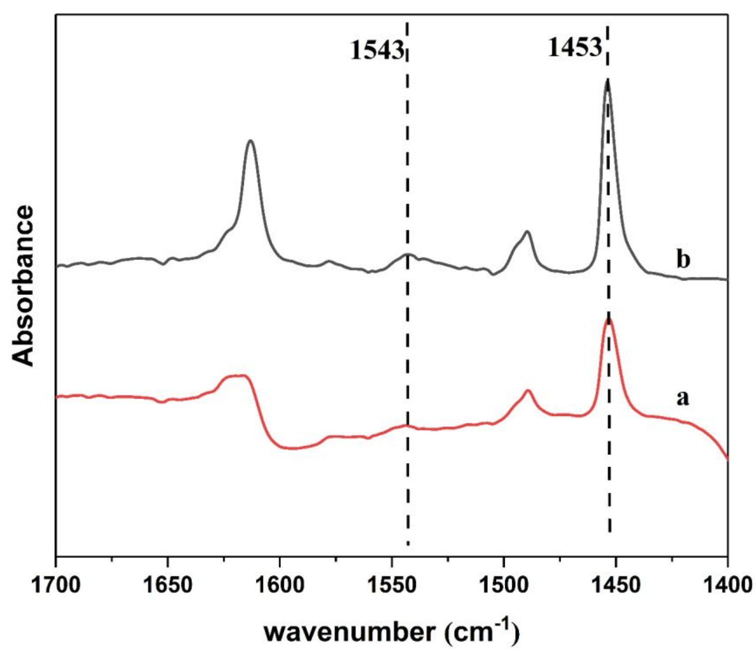

Figure S5. Py-IR spectra of (a) spend catalyst FZ-PSA18, (b) fresh catalyst FZ-PSA18

Table S3. B acid, L acid and Total acid of fresh catalyst FZ-PSA18 and spend catalyst FZ-PSA18

Catalysts	Total acid sites (μmol/g)			Medium and strong acid sites (μmol/g)		
	B	L	Total	B	L	Total
fresh catalyst FZ-PSA18	20	149	169	14	72	86
spend catalyst FZ-PSA18	8	74	82	4	49	53

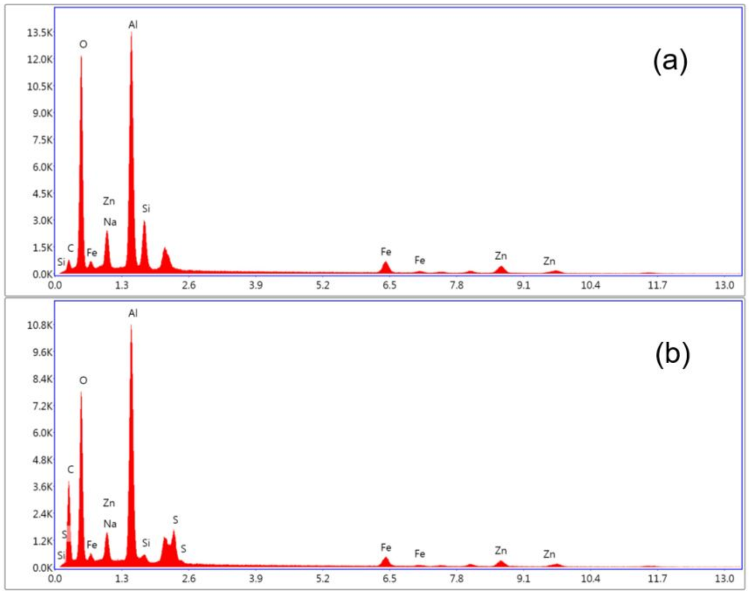

Figure S6. SEM-EDS spectra of catalysts. (a) fresh catalyst FZ-PSA18, (b) spend catalyst FZ-PSA18